Experimental investigation of the confinement effect on a flame impinging a ceiling in an enclosure

Aijuan Wang, Brady Manescau, Khaled Chetehouna, Charles de Izarra, Steve Rudz

Version of Record: https://www.sciencedirect.com/science/article/pii/S0379711221000850
Manuscript_003f9ef8520f613c0068e35eef34abbb

Experimental investigation of the confinement effect on a flame impinging a ceiling in an enclosure

A.J. Wang[a], B. Manescau[a], K. Chetehouna[a,*], C. De Izarra[a], S. Rudz[b]

[a] *INSA Centre Val de Loire, Univ. Orléans, PRISME, EA 4229, F-18022 Bourges, France*
[b]*GREMI, UMR 7344, Université d'Orléans/CNRS, F-18020 Bourges, France*

Abstract

This experimental study highlights the confinement effects on a flame impinging a ceiling in confined or semi-confined environment. The enclosure used in this study represents a 1:10 scale model of a student compartment with two possible openings: a door and a window. It is developed based on the conservation of the Froude number based on the scaling law. The objective of this work is to provide explanations in terms of fire safety on thermal phenomena that can occur during fires in closed environments, for example in a room of a university residence, regarding eight heat rates release of fuel and five confinement levels. A flame oscillation modelling of propane-air flame is proposed and is verified by the experimental results. It is shown both by theoretical modeling and experimental results that the confinement of a compartment has an effect on period time of flame oscillation. Moreover, experimental results show that the confinement level of compartment is a key parameter to characterize vertical temperature evolution both in the center (impinging zone) and near the wall in the enclosure. The correlations for normalized gas temperature rise near the wall are proposed and these temperature evolutions are bounded by the ventilation conditions of the five configurations. Indeed, under condition of equivalence ratio greater than 1, the maximum gas temperature near the wall of a certain heat release rate decreases dramatically with the increasing of confinement level of configurations, which is associated to the decrease in flame intensity by lack of oxygen with a great criterion of under ventilation.

* Corresponding author.
E-mail address： *khaled.chetehouna@insa-cvl.fr.*

Keywords: Confinement level, Impinging flame, Temperature distribution, Equivalence ratio, Fire safety

1. Introduction

In a burning enclosure, flame can extend along a ceiling that contributed to the dramatically increase of heat flux and temperature on the ceiling [1,2]. With the heat transfer through the ceiling, fire can spread from one room to another: unacceptable situation for fire safety engineering [3]. Consequently, the behavior of flames impinging ceilings and thermal gradients observed in closed or semi-closed environments are of great interest to fire safety engineering [4,5].

The flame-wall interaction in an open or semi-confined environment has been studied earlier [3,6–8] and was also an ongoing topic over the last decades [9–17]. In the objective to characterize the behavior of flame impinging a ceiling in open environment, several models for predicting physical parameters such as the temperature profile under the ceiling have developed by many works [3,6–8]. Among these models, McCaffrey [6] proposed that the vertical temperature profile of buoyant turbulent flame could be divided into three regions: continuous flame region, intermittent flame region and plume region. The relations for each region were developed and validated by the experimental results. In the same context, Heskestad and Hamada [1] developed a correlation for temperature rise under ceiling which was caused by the impinging plume of a solid fuel. Alpert [7] predicted the major characteristics of the turbulent ceiling-jet fire as functions of heat release rates and distance beneath the ceiling, which were in consideration of the air entrainment model. This correlation was then improved by Li et al. [11] and Ji et al. [12] for flame impinging on a confined ceiling. Ji et al. [12] carried out series of experiments in a small-scale (1:6) urban road tunnel with fire located in different distances to the sidewall and found that the maximum smoke temperature under the ceiling in the tunnel larger than in the unconfined space, owing to the restriction effect. In consideration of multiple fire sources, Wan et al. [17] investigated gas temperature distribution under unconfined ceiling impinged by two fire sources. They showed that the interaction between multiple flames might lead to flames tilt to each other and even merge together with small spacings, resulting in different ceiling gas temperature distribution in comparison with the case of a flame.

Furthermore, it was shown that the behavior of flame impinging a ceiling is greatly influenced by the geometry of walls (corridor, corner…) [18–25]. For this reason, Gao et al. [21] carried out a series of experiments in the 1/6 scale tunnel model, of which fire source was located near the sidewall. Similar to the free plume [6], the centerline ceiling temperature was also can be divided into three regions but the ceiling temperature was closely in relation to the effective heat release rate not the total heat release rate. Different from

the horizontal ceiling, Zhang et al. [22] performed experiments of a wall confined flame impinging on an inclined ceiling. They found that the inclination angle of ceiling didn't affect remarkably on the maximum temperature rise under the ceiling in the flame impingement region and a new relation was proposed to predict the temperature decay profiles by taking the ceiling angle into account. In addition, Zhao et al. [25] studied the effects of openings on fire properties of the ceiling-jet in a confined reduced-scale corridor using both experimental and numerical methods. With the varying of the size and position of opening, the mass lose and temperature field were measured and compared to Delichatsios's model and previous studies while the influence mechanism of openings wasn't revealed.

In the works cited above, the major part studied the behaviour of the impinging flame in a completely open environment and minor works presented the behaviour of impinging flame in a semi-closed condition. However, there is rarely work that focuses on the effect of the confinement level of the configurations on impinging flame [25], for example flame impinging a ceiling of compartments. Indeed, in consideration of the windows and doors of a compartment, it is possible to produce different confinement levels. Thus, the fire dynamics and thermal behaviour of a flame impinging a ceiling will strongly depend on the confinement level of the compartment. In order to provide explanations related to this subject, this work studies the confinement effects on the temperature distribution and flame oscillation in a burning enclosure. The experimental device used is a small-scale compartment (1:10) representing a student compartment model in the university residence. The design of this model was carried out by conserving the Froude number based on the scaling law. The experimental tests were carried out for five configurations with eight heat release rates. By coupling the different openings conditions with the heat capacities used in this study, confinement levels are connected to the equivalence ratio in the compartment. In addition, the results in this work can be used as a mean of evaluating thermal effects which can contribute to the fire spread in compartments.

2. Experimental details

2.1. Experimental setup

The experimental setup used in this study is presented in Fig. 1. It is a compartment at small-scale (1:10), whose dimensions are 0.6 m (length) × 0.4 m (width) × 0.24 m (height) with one door and one window. Based on a survey of the single room in France, England, Australia and other countries, it is found that, generally, the area of single room in different countries is in the range of 15-30 m^2. For this, the area of the large-scale

compartment is equal to 24 m^2 and it particularly represents a student room in university residence. The small-scale compartment was then developed according to the scaling law based on the conservation of the Froude number [26]. The dimensions of the window are 0.15 m (height) × 0.15 m (width) and the dimensions of the door are 0.20 m (height) × 0.09 m (width). The sidewalls of the enclosure are made of fireproofing concrete plate with a thickness of 2 cm and the ceiling is made in steel plate. Their thermal properties are presented in Table 1:

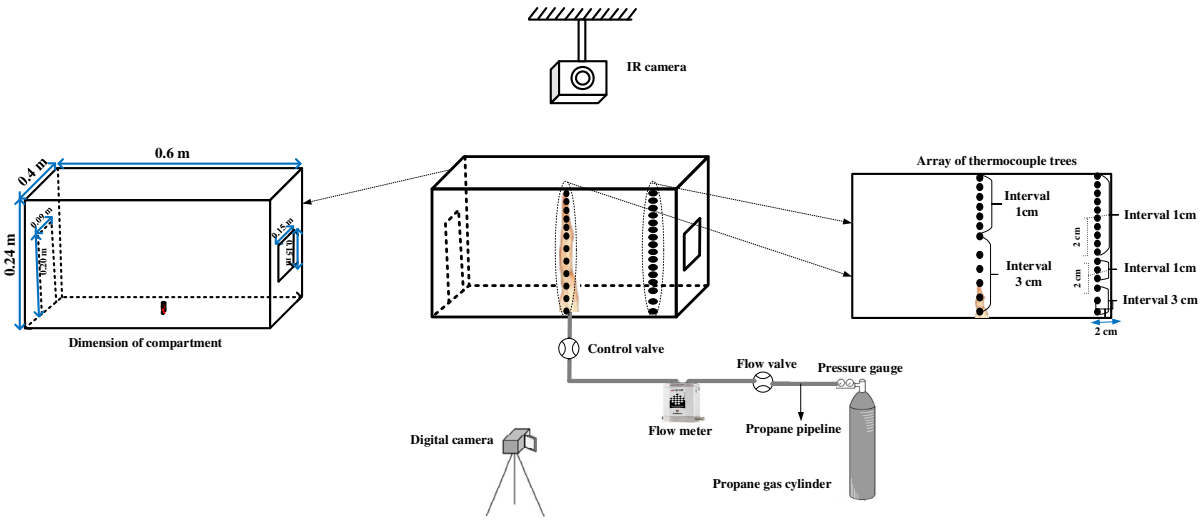

Fig. 1. Schematic of the experimental set up

Table 1. Thermal parameters of aerated concrete and steel

Thermal parameters	Aerated concrete	Steel
Density (kg/m^3)	870	7850
Conductivity (W/mK)	0.175	46
Specific heat ($kJ/kg \cdot K$)	0.92	0.5

In this work, the fire source was provided by a gas burner with the nozzle's diameter of 5 mm, which was placed in the center of the compartment. The fuel used was the propane (C_3H_8) with a heat of combustion of 46.45 kJ/g. The mass flow rate of fuel was controlled by a Bronkhorst Coriolis mass flow meter with a range of 0-1.00 g/s with an accuracy of 0.05 g/s. The used instrumentations were an infrared camera, K-type thermocouples and a digital camera. The infrared camera (IR) was a FLIR A655sc which can record field temperature from -45 °C to 2000 °C with a frequency of 35 frames per second. It was set above the ceiling at 2 m of the target with an emissivity and a transmission of 1. It measured the temperature field on the ceiling. Two columns of K-type stainless thermocouples were placed in the center and near sidewall from floor to ceiling, respectively. Flame videos were recorded by a digital camera (DV) with a frequency of 25 frames per second, that was set 1 m in front of the target. The flame videos were further processed by the image processing method, which included three consecutive steps: direct linear transformation (DLT), fire segmentation and flame length

computation. More details on this methodology are presented in a previous work [27]. The uncertainty of the measurements was mainly attributed to the error due to thermocouple radiation and the error related to measurement repeatability. Each test was conducted three times to ensure reproducible results within permitted error ranges.

In this work, the Froude number modeling was applied to build up the physical scale model. With the conservation of Froude number, the scaling law between reduced-scale and full-scale model can be obtained. Based on the geometric scale, temperature scale and heat release scale, physical parameters such as geometry L, temperature T, and heat release rate $\dot{Q}$ can be scaled with the following Eqs. (1)(2)(3):

$$\bar{L} = \frac{L_R}{L_F} \tag{1}$$

$$T_R = T_f \tag{2}$$

$$\bar{\dot{Q}} = \frac{\dot{Q}_R}{\dot{Q}_F} = (\bar{L})^{5/2} \tag{3}$$

where the subscript 'R' and 'F' denote the reduced-scale model and full-scale model respectively.

2.2. Test series

In order to highlight the confinement effect, five different configurations were used with the different opening conditions of door and window (Ref. Table 2). Thus, the confined factor, δ_c of each configuration can be calculated based on the opening factor proposed by Pettersson et al. [27]:

$$\delta_c = 1 - \frac{A_o\sqrt{H_o}}{A_t\sqrt{H_t}} \tag{4}$$

where δ_c represents the confined factor, A_o is the area of opening, A_t is the area of the total compartment, H_t is the height of the compartment, H_o is the height of the opening. For Conf. 2, $A_o = A_d + A_w$ and $H_o = (A_d h_d + A_w h_w)/A_o$ [27].

In this work, Conf. 5 is assumed completely confined with the neglection of leakages. Thus, the experimental configurations with the confined factor are summarized in Table 2. It can be seen that the confinement level increases from Conf. 1 to Conf. 5.

Table 2. The experimental configurations with the confined factor

Configurations	Condition of openings		A_o	$\sqrt{H_o}$	δ_c
	Window	Door			
Conf. 1	Flame impinging a ceiling in open environment		∞	-	0
Conf. 2	Open	Open	0.0405	0.415	0.964
Conf. 3	Open	Closed	0.0225	0.387	0.981
Conf. 4	Closed	Open	0.0180	0.447	0.983
Conf. 5	Closed	Closed	≈0	-	≈1

In each series of experiments, eight different heat release rates (HRRs) have been used: HRRs = {0.5, 1.2, 2.3, 4.6, 9.3, 14.0, 16.3, 18.6} kW. These HRRs represent the different heat capacities that it is possible to get in the experiments, set up in relation to the compartment in real scale.

In order to study the confinement effects on the behavior of the flame impinging the ceiling, the equivalence ratio is used. This makes it possible that depending on its value, to indicate the confinement level related to the mass flow rates of the fuel released. The equivalence ratio is defined as following:

$$\varphi = \frac{fuel-to-oxidizer\ \text{ratio}}{(fuel-to-oxidizer\ \text{ratio})_{st}} = \frac{m_{fuel}/m_{ox}}{(m_{fuel}/m_{ox})_{st}} \tag{5}$$

The calculation of this parameter is based on the ratio between the quantity of fuel (propane) which reacts with the oxidizer (air) illustrated in Eq. (5). In this study, it was possible to determine the quantity of fuel (propane) released into the enclosure after a test period (120 s). Concerning the estimation of the quantity of air which reacted, this was determined by the quantity of air contained in the volume of the enclosure. For the calculation of the equivalence ratio, configuration 5 which represents the completely closed enclosure was used as a reference to calculate this parameter. Additionally, based on the measurements of the O_2 concentration remaining after each test, it was found that only about half of the oxygen reacted in the study scenarios. The calculation of the equivalence ratio was carried out by considering the quantity of fuel released after 120 s and half quantity of air present in the enclosure. Moreover, the combustion of the propane was carried out in good condition with the minimum oxygen concentration of 10.5 %, representing half of the oxygen concentration in air. For that, the calculation of the equivalence ratio is made using the half amount of air calculated from the volume of the enclosure.

The equivalence ratio of the complete confined configuration, i.e. Conf. 5, is used as the reference equivalence ratio. From the calculations, equivalence ratio φ of Conf. 5 with eight HRRs is shown in Table 3. It can be seen that, equivalence ratio is between 0.12 and 4.70, and the equivalence ratio is larger than 1 for heat release rate larger than 4.6 kW.

Table 3. Equivalence ratio φ of Conf. 5 under eight HRRs

HRR (kW)	0.5	1.2	2.3	4.6	9.3	14.0	16.3	18.6
φ	0.12	0.29	0.59	1.17	2.35	3.52	4.11	4.70

3. Flame oscillation modeling of a propane-air diffusion flame

In Refs. [28–31], the evaluation level of the oscillation of a diffusion flame can be obtained from the mass flow rate of the fuel. In the current study, the fuel is the propane.

It is possible to define two typical time scales that give rise to flame oscillations: the convection time scale and the diffusion time scale [32]. From the typical flame radius R_f and the gas diffusion coefficient D_{iff}, it is possible to evaluate the typical diffusion time τ_{diff} of the flame oscillations by the following relation [33]:

$$\tau_{diff} = \frac{R_f^2}{D_{iff}} \tag{6}$$

The typical convection time τ_{conv} is given by the following relation:

$$\tau_{conv} = \frac{L_f}{u_0} \tag{7}$$

where L_f is the flame length and u_0 is the speed of the flame jet.

One of our typical experimental conditions are as follows: mass flow rate of propane $\dot{m} = 0.1\ g/s$ ($u_0 = 2.1\ m/s$), flame radius R=1 cm, flame length $L_f = 46\ cm$ and the diffusion coefficient is $D_{iff} = 0.1\ cm^2/s$. With these values, typical diffusion and convection times are:

$$\tau_{conv} = 0.22\ \text{s} \tag{8}$$

$$\tau_{diff} = 10\ \text{s}$$

Knowing that, the temporal fluctuations observed are of the order of ten seconds, we decide to take into account only the diffusion phenomenon, with a differential delay equation [29].

In order to dissociate from the complex phenomena, present in the reaction zone of the flame, only the zone of the flame where there is no combustion will be considered. With this assumption, the typical times of

chemical reactions are much lower than the typical times of diffusion. We will therefore consider oxygen as the diffusion gas. We define the variation in oxygen concentration using the following relationship (Fick's law):

$$\frac{dx}{dt} = \frac{D_{iff}}{R_f^2}\left(x_0 - x(t)\right) \tag{9}$$

where $x(t)$ is the oxygen concentration at time t, D_{iff} is the oxygen diffusion coefficient, R_f is the flame radius and x_0 is the oxygen concentration outside of the flame.

Since the diffusion of oxygen is not instantaneous, we introduce a delay τ in the previous differential equation [29], that becomes:

$$\frac{dx}{dt} = \frac{D_{iff}}{R_f^2}\left(x_0 - x(t-\tau)\right) \tag{10}$$

and using the 2nd order approximation of Taylor expansion of $x(t-\tau)$:

$$x\left(t-\tau\right) = \sum_{k=0}^{\infty} \frac{\left(-\tau\right)^k}{k!} x^{(k)}\left(t\right) \approx x\left(t\right) - \frac{\tau}{1!}\frac{dx}{dt} + \frac{\tau^2}{2!}\frac{d^2x}{dt^2} + \ldots \tag{11}$$

It is deduced:

$$\frac{d^2x}{dt^2} + \frac{2R_f^2}{D_{iff}\tau^2}\left(1 - \frac{D_{iff}\tau}{R_f^2}\right)\cdot\frac{dx}{dt} + \frac{2}{\tau^2}x = \frac{2x_0}{\tau^2} \tag{12}$$

From the flame fluctuations observed experimentally, we will hypothesize that the problem is reduced to that of a harmonic oscillator with:

$$\frac{d^2x}{dt^2} + 2\lambda\frac{dx}{dt} + \omega_0^2 x = \frac{2x_0}{\tau^2} \tag{13}$$

In this context, we decide to put the friction term $\frac{2R^2}{D\tau^2}\left(1 - \frac{D\tau}{R^2}\right).\frac{dx}{dt}$ to zero:

$$\frac{2R_f^{22}}{D_{iff}\tau^2}\left(1 - \frac{D_{iff}\cdot\tau}{R_f^2}\right) = 0 \Rightarrow \tau = \frac{R_f^2}{D_{iff}} \tag{14}$$

In addition, the third term $\omega_0^2 = 2/\tau^2$ of the Eq. (13) can be associated with the frequency of oscillation of the flame, so we can determine the frequency by the following relationship:

$$\omega_0^2 = \frac{2}{\tau^2} \Rightarrow \omega_0 = \frac{\sqrt{2}}{\tau} \tag{15}$$

Since ω_0 is linked to the period of flame oscillation T_{os}, we have:

$$T_{os} = \frac{2\pi}{\omega_0} \Rightarrow T_{os} = \frac{2\pi \cdot \tau}{\sqrt{2}} = \sqrt{2} \cdot \pi \cdot \tau \tag{16}$$

At the last, using Eq. (14):

$$T_{os} = \sqrt{2} \cdot \pi \cdot \frac{R_f^2}{D_{iff}} \tag{17}$$

This expression represents the oscillation period of the flame. As gas diffusion coefficient D_{iff} depends on the temperature, so that flame oscillation is related to the temperature in the compartment.

4. Results and discussion

4.1. Flame oscillations in confined compartment

Fig. 2 depicts the experimental measurements of the mean flame length over time for Conf. 2, i.e. impinging flame in compartment of open door and window, with HRR=4.6 kW. It can be seen that flame fluctuates with a period time about the order of 10 seconds. These measurements were obtained from video recordings that lasted approximately 120 seconds (see Fig. 2).

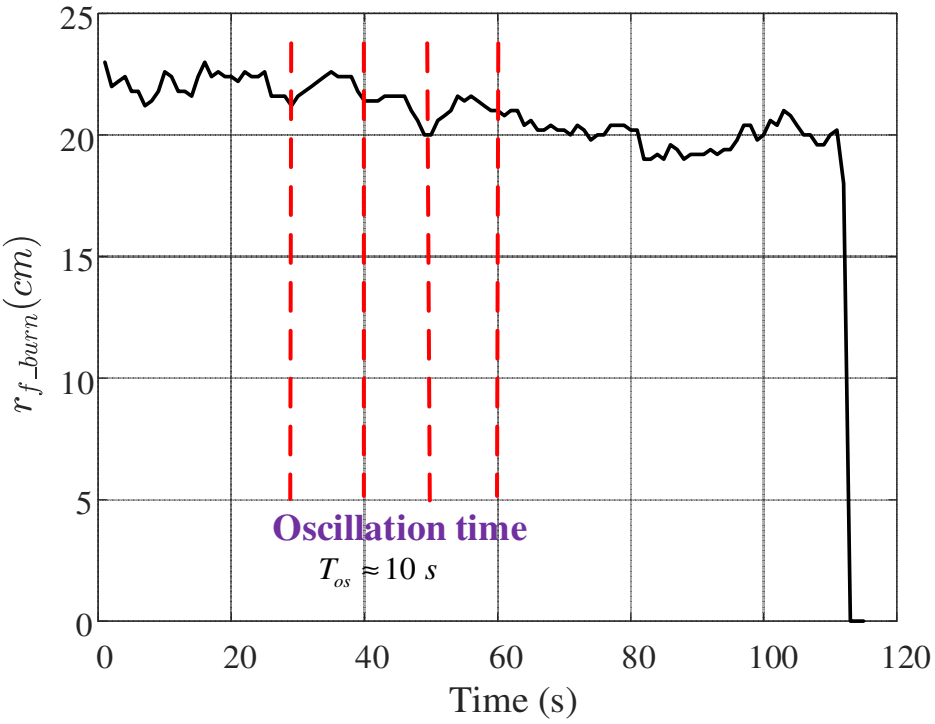

Fig. 2. Mean flame length over time for Conf. 2 with HRR=4.6 kW

In order to apply Eq. (17), that gives the period from the differential equation delay model, the diffusion coefficient must be evaluated more precisely. The kinetic theory of gases establishes that D_{iff} varies as a

function of temperature according to $D_{iff} \propto T^{3/2}$ [33]. Considering flame temperature between 600°C and 800°C, the diffusion coefficient of oxygen in propane is of the order of $D_{iff} \approx 0.5\ cm^2/s$. The application of Eq. (17), gives an oscillation period $T = 8.9\ s$, which is agreement with the measurements obtained in the current work.

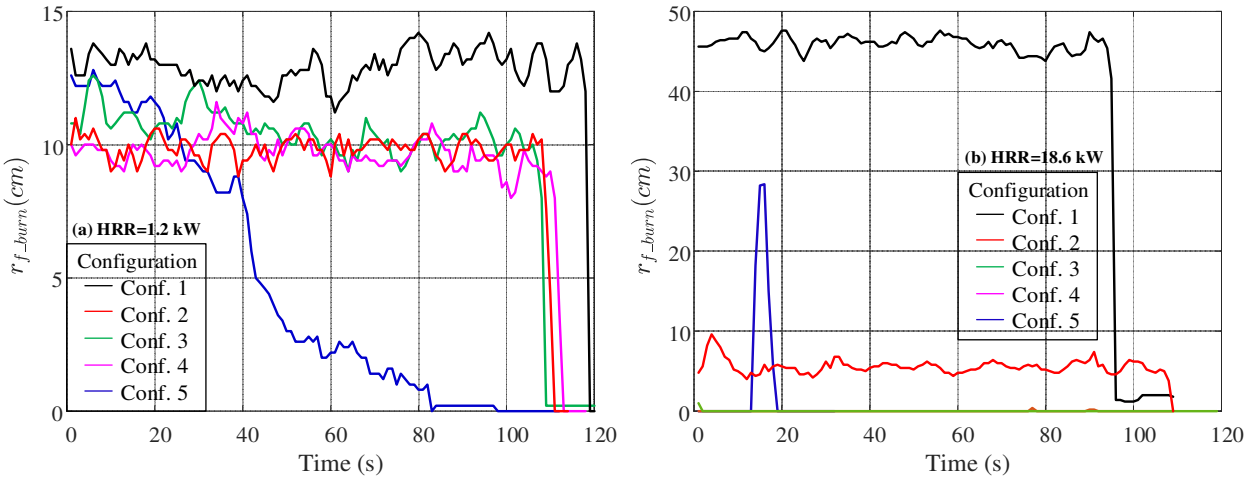

Fig. 3. Mean flame length over time for five configurations with: (a) HRR=1.2 kW; (b) HRR=18.6 kW

Fig. 3 shows the experimental measurements of mean flame length over time for five configurations with HRR=1.2 kW and HRR=18.6 kW, which are respectively the minimum and maximum HRRs in this study. It is shown that in Fig. 3 (a), the confinement level of the configurations has a little effect on the flame oscillation time as the equivalence ratios of five configuration are smaller than 1.

However, it can be seen from Fig. 3 (b), flame oscillation time varies greatly with the confinement level of the configurations. When HRR=18.6 kW, the equivalence ratio of each configuration is greater than 1. In this condition, flame temperature decreases with the decrease in flame intensity due to the lack of oxygen in the enclosure. For it, the more the confinement level increases, the more the flame temperature decreases, even leading to the extinction of the flame.

4.2. Confinement effect on vertical temperature distribution in impinging zone

The fire plume in open space is conventionally divided into three zones: continuous flame zone, intermittent flame zone and buoyant plume zone [6]. For flame impinging a ceiling, Gao et al. [13] has pointed that the ceiling excess temperature of 400 K and 600 K can be considered as two critical values to evaluate the impinging condition under the ceiling. For $\Delta T < 400\ K$, $400\ K < \Delta T < 600\ K$ and $\Delta T > 600\ K$, they represent buoyant plume, intermittent flame and continuous flame respectively.

Fig. 4 shows the vertical temperature distribution in impinging zone for five configurations with the varying eight heat release rates from 0.5 kW to 18.6 kW. It can be seen that for Conf. 1, i.e. flame impinging a ceiling in open environment, the vertical excess temperature ΔT increases with the height above fire source, owing to the flame progress with the increasing of burning rate. It should be noted that for Conf. 1, even the excess temperature near the ceiling is greater than 600 K in condition of all eight heat release rates, which means that the flame is continuous under the ceiling. Furthermore, for Conf. 1, the ceiling is impinged by a strong plume with all heat release rates of the gas burner from 0.5 kW to 18.6 kW. Specially, the plume under the ceiling is in the first zone of plume: continuous flame zone, such that it's called impinging flame in this work.

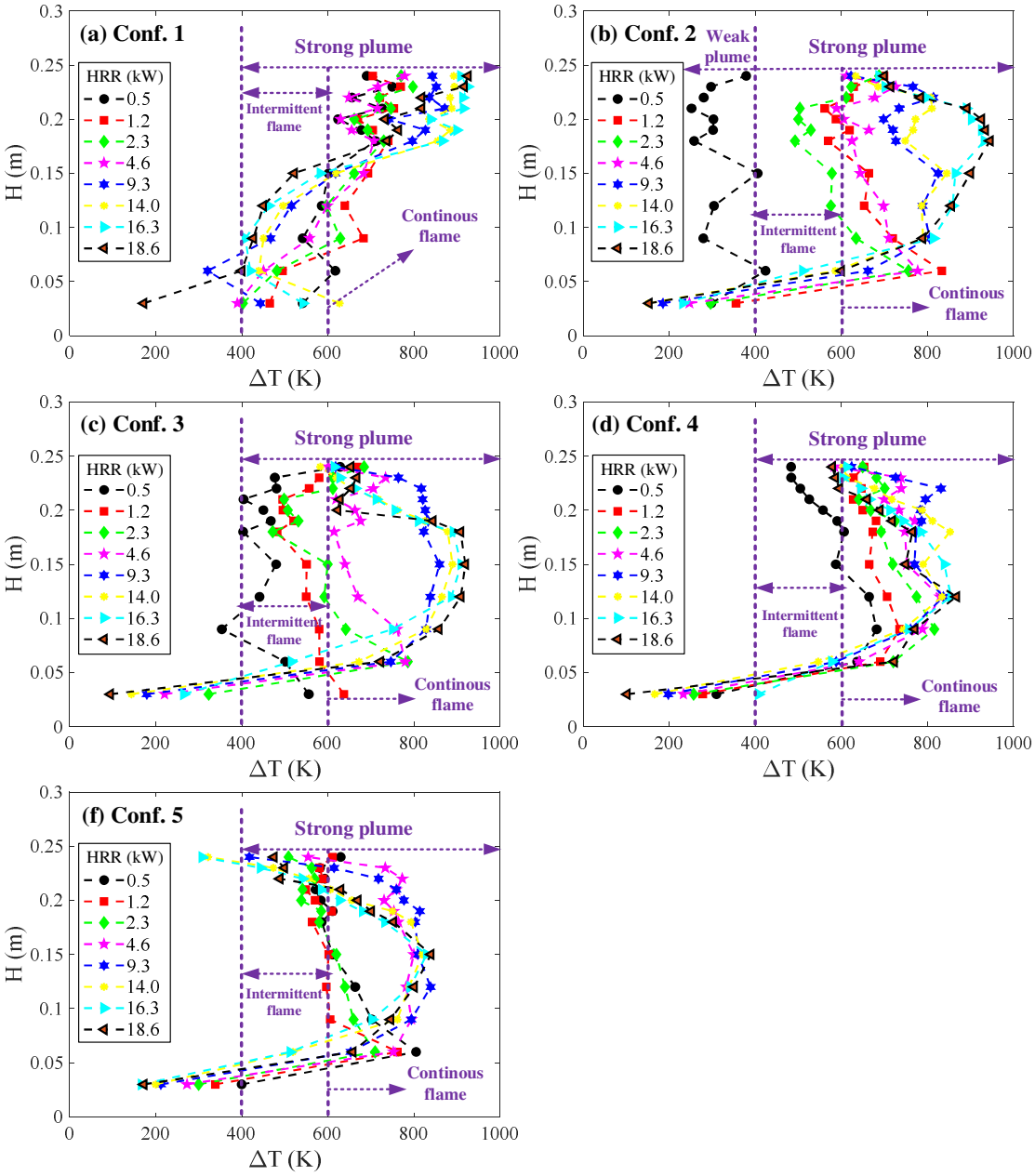

Fig. 4. Vertical temperature distribution in impinging zone for five configurations

For a strong plume, Ji et al. [34] proposed a correlation for predicting the ΔT_{max} under a confined ceiling:

$$\frac{\Delta T_{\max}}{T_\infty} = \begin{cases} 0.267\dfrac{\dot{Q}^{2/5}}{H}, & \dfrac{\dot{Q}^{2/5}}{H} < 10.9 \\ 2.9, & \dfrac{\dot{Q}^{2/5}}{H} \geq 10.9 \end{cases} \tag{18}$$

In Eq. (18), the two parts are consistent with the intermittent and continuous impinging flames respectively.

As discussed above, the impinging plumes in this work are considered to be strong plumes with intermittent and continuous impinging flames under the ceiling. Thus, an equation for predicting maximum

temperature rise in impinging zone ΔT_{max} for Conf. 1, i.e. flame impinging a ceiling in open environment, is proposed:

$$\frac{\Delta T_{\max}}{T_\infty} = \begin{cases} 0.06\dfrac{\dot{Q}^{2/5}}{H} + 2.4, & \dfrac{\dot{Q}^{2/5}}{H} < 12.7 \\ 3.1, & \dfrac{\dot{Q}^{2/5}}{H} \geq 12.7 \end{cases} \tag{19}$$

The experimental data and fitted curve for nondimensional maximum temperature rise in impinging zone for Conf. 1 are presented in Fig. 5.

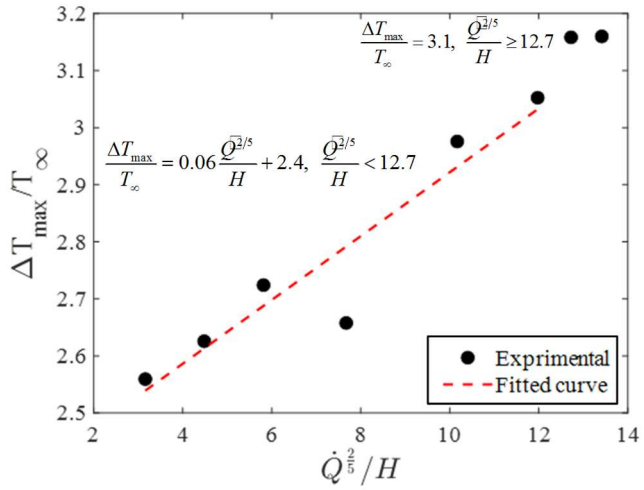

Fig. 5. The experimental data and fitted curve for nondimensional maximum temperature rise in impinging zone

4.3. Confinement effect on vertical temperature distribution near the wall

Fig. 6 shows the vertical gas temperature near the wall for eight HRRs. On reading these graphs, it is shown that for HRRs less than 4.6 kW, the vertical temperature evolution under the ceiling is similar for all configurations while the maximum temperature under the ceiling for confined configuration (i.e. Conf. 2 to Conf. 5) are higher than the flame impinging a ceiling in open environment (i.e. Conf. 1) owing to the heat accumulation in the compartment.

However, they show differences for the heat release rates of 9.3 kW, 14.0 kW, 16.3 kW and 18.6 kW (Fig. 6 (e)(f)(g)(h)), which corresponds to equivalence ratio larger than 1. At a certain HRR, for example HRR=14.0 kW, the maximum gas temperature of configuration decreases when the confinement level of configuration increases. It is noted that these maximum temperatures decrease to converge towards the values of temperature in the lower part of the room. Indeed, the more the confinement level increases, the more the accumulation of smoke rich in unburnt gases. These smoke layers thicken from the ceiling to the ground, promoting temperature

uniformity in the room when the flame intensity decreases due to the lack of oxygen in the compartment. For HRRs larger than 9.3 kW (equivalence ratio larger than 1) (Fig. 6 (f)(g)(h)), the temperature evolutions are similar considering the presence of flame fluctuation.

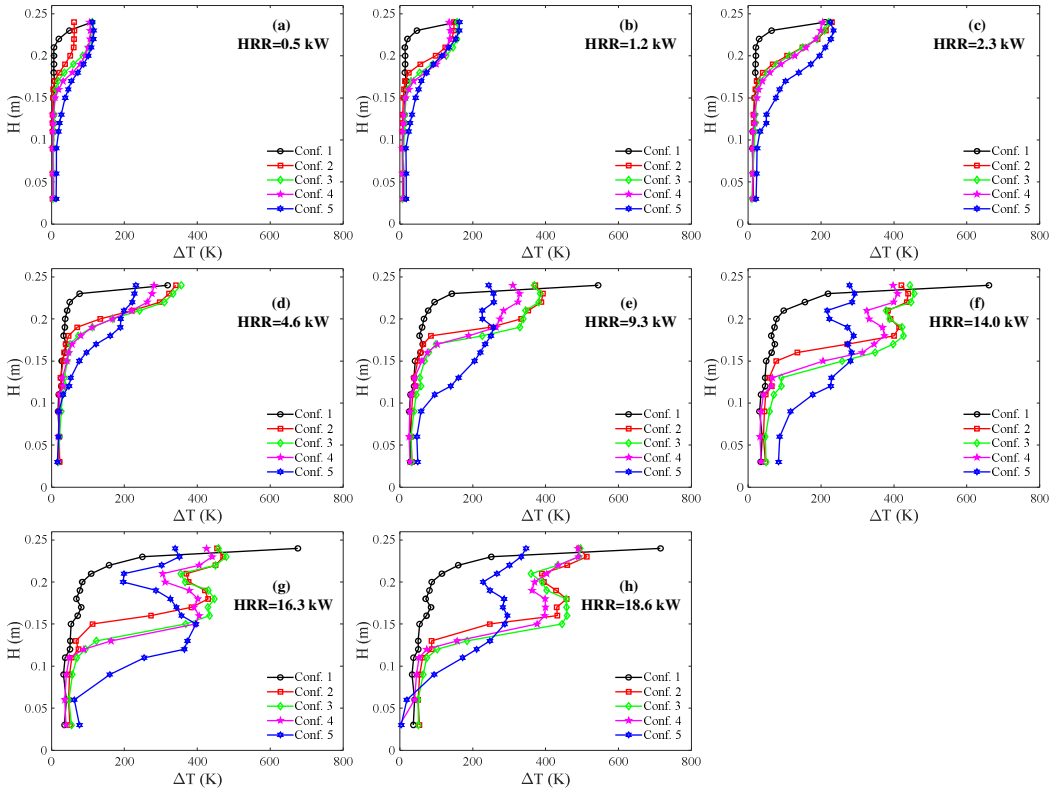

Fig. 6. Vertical gas temperature distribution near the wall for eight HRRs

Fig. 7 shows maximum gas temperature rise under ceiling (ΔT_{max}) against $\dot{Q}$. It is clear that the maximum temperature rise under ceiling of Conf. 1 increases with the increasing of $\dot{Q}$. For heat release rates less than 4.6 kW, the ΔT_{max} presents nearly unchanged for all configurations. The HRR of 4.6 kW presents a turning point of the maximum temperature rise in five configurations (Conf. 1 to Conf. 5). For heat release rates larger than 4.6 kW, which is corresponding to equivalence ratio larger than 1, the maximum temperature gap between Conf. 1 and Conf. 5 increases dramatically with the increasing of heat release rate, from 87 K to 369 K. That is associated to the decrease in flame intensity by lack of oxygen with the increasing in confinement level of configurations. Thus, from the results presented in this study, it is shown that the flame intensity decreases as a function of the compartment's confinement level.

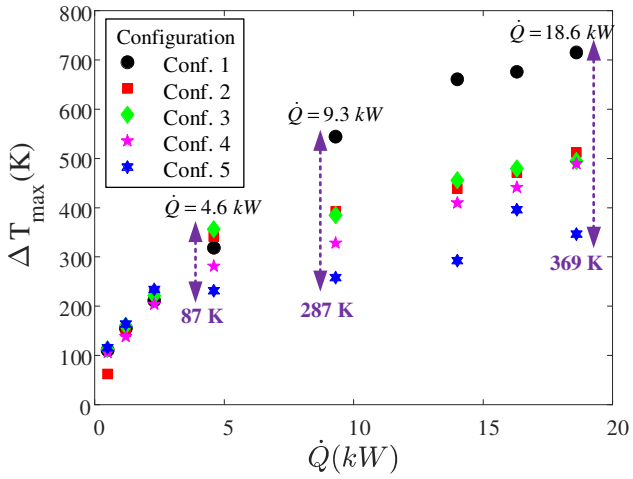

Fig. 7. Maximum gas temperature rise near the wall (ΔT_{max}) against $\dot{Q}$

Fig. 8 shows relationships between normalized temperature rise and normalized HRR for five configurations, which are obtained by the fitting of experimental data. It can be seen that with the increasing of normalized HRR, normalized temperature rise increases for all five configurations. Indeed, at a certain $\dot{Q}^*$, especially for $\dot{Q}^*$ larger than 2.2×10^3, which corresponds to the equivalence ratio larger than 1, normalized temperature rise decreases with the increasing of confinement level. These temperature evolutions are bounded by the ventilation conditions of the five configurations. Correlations of normalized temperature rise for five configurations are listed in Table 4.

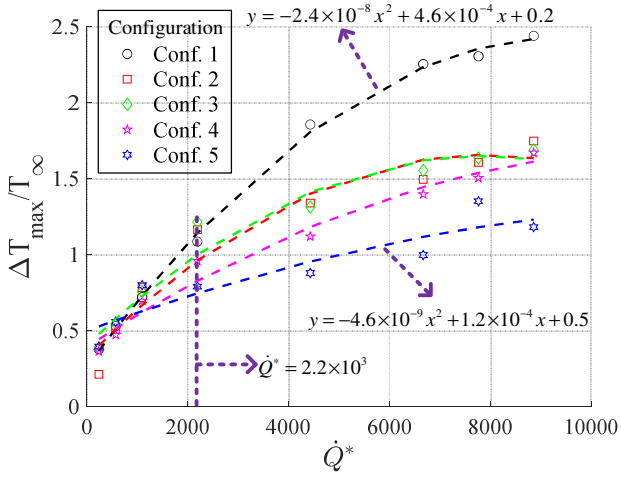

Fig. 8. Relationships between normalized gas temperature rise and normalized HRR for five configurations

Table 4. Correlations of normalized temperature rise for five configurations

Configuration	Correlations	
Conf. 1	$\frac{\Delta T_{max}}{T_\infty} = -2.4\times10^{-8}\dot{Q}^{*2} + 4.6\times10^{-4}\dot{Q}^{*} + 0.2$	(20)

Conf. 2 $$\frac{\Delta T_{max}}{T_\infty} = -2.2\times10^{-8}\dot{Q}^{*2} + 3.4\times10^{-4}\dot{Q}^{*} + 0.3 \quad (21)$$

Conf. 3 $$\frac{\Delta T_{max}}{T_\infty} = -2.0\times10^{-8}\dot{Q}^{*2} + 3.2\times10^{-4}\dot{Q}^{*} + 0.4 \quad (22)$$

Conf. 4 $$\frac{\Delta T_{max}}{T_\infty} = -9.2\times10^{-9}\dot{Q}^{*2} + 2.2\times10^{-4}\dot{Q}^{*} + 0.4 \quad (23)$$

Conf. 5 $$\frac{\Delta T_{max}}{T_\infty} = -4.6\times10^{-9}\dot{Q}^{*2} + 1.2\times10^{-4}\dot{Q}^{*} + 0.5 \quad (24)$$

$$\dot{Q}^{*} = \frac{\dot{Q}}{\rho_\infty T_\infty c_p \sqrt{g D^5}}$$

4.4. Confinement effect on horizontal temperature decay on the ceiling

Fig. 9 shows temperature fields on the ceiling for different confinement levels at HRR of 9.3 kW, obtained by IR camera which can represent the flame impinging zone on the ceiling. The imping zones are almost symmetrical because the conditions of fire in enclosure are near symmetrical even through the confinement levels are relatively high.

It is possible to observe the confinement effects by the yellow area impinged by the flame and the red area impinged by the plume. It is clearly visible that the flame impinging area decreases and the plume impinging area increases with the increasing of configurations' confinement level, i.e. from Conf. 2 to Conf. 5.

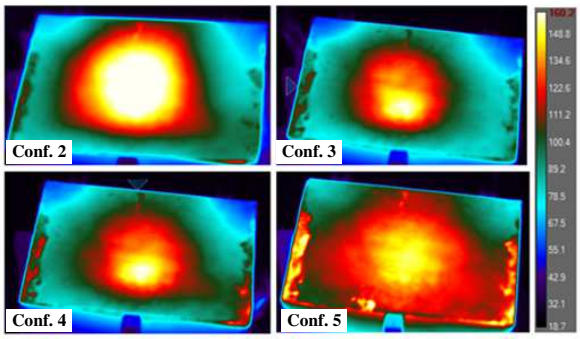

Fig. 9. Temperature fields on the ceiling for different confinement levels at HRR of 9.3 kW

Fig. 10 depicts the temperature distribution along the transverse radius of ceiling for four confined configurations with the HRRs increasing from 1.2 to 18.6 kW: these measurements are obtained using the IR camera. It is shown that the maximum ceiling temperature is at the flame impinging point and decreases along the transverse radius of ceiling.

Also, in Fig. 10 (a), it represents the configuration of impinging flame in the compartment with open window and door (Conf. 2). It can be seen that the temperature amplitude on the ceiling increases with the increasing of HRRs. However, for other more confined configurations (Conf. 3, Conf. 4 and Conf. 5), the temperature amplitude on the ceiling is not monotonously increased with the increasing of HRRs. Particularly for the most severe confined configuration, i.e. Conf. 5, the temperature amplitude with HRR of 18.6 kW converges to temperature amplitude with HRR of 1.2 kW.

Note that in Conf. 5, the temperature decays slightly along the transverse radius of ceiling for larger HRRs (HRR > 9.3 kW, φ >1). This can be caused by the incomplete combustion in the enclosure so that the total enclosure is filled with the unburn gas and smoke. The dangerous accidents such as backdraft and flashover may occur if a window or door is broken manually or automatically in these conditions.

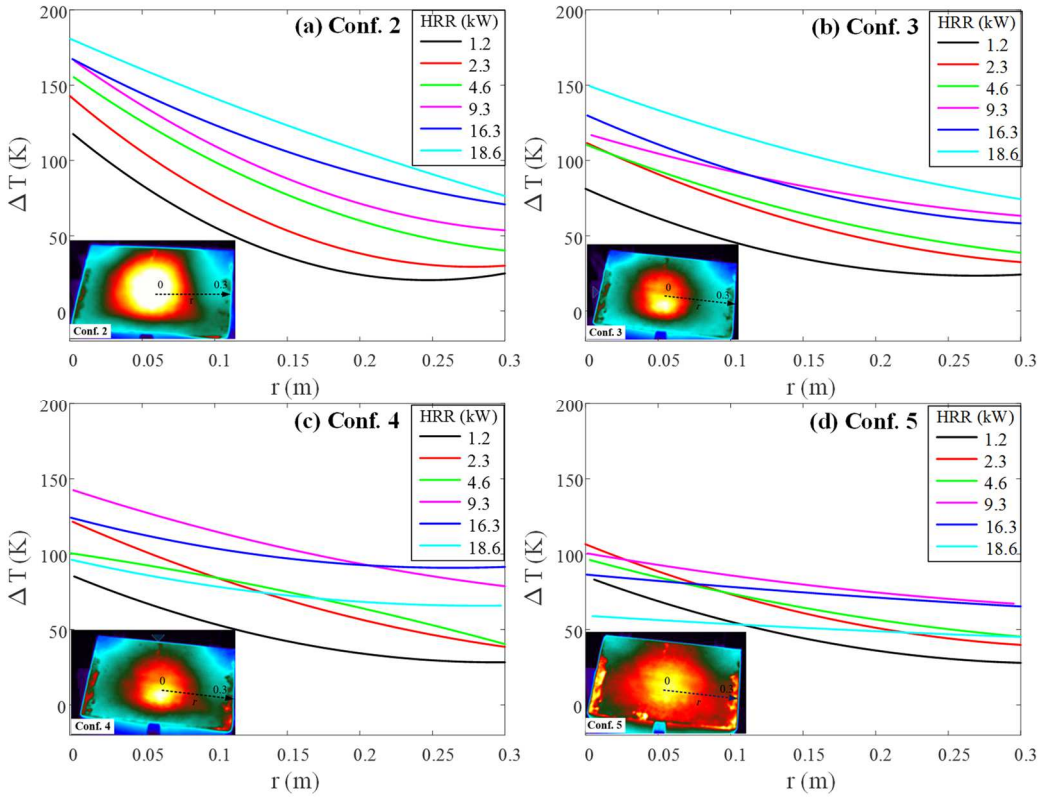

Fig. 10. Temperature distribution along the transverse radius of ceiling

5. Conclusions

The aim of this work is to investigate the confinement effects on fire dynamics and heat transfer for impinging flame in the enclosure. For obtaining this object, a small-scale (1:10) compartment model has developed. A systematic experimental study is performed using five configurations with eight heat release rates,

on the temperature distributions of impinging zone, smoke layer and ceiling's surface, as well as flame oscillation. The major findings include:

(1) A flame oscillation modelling of a propane-air flame is proposed and is verified by the experimental results. It is shown both by theoretical modeling and experimental results that confinement level of a compartment has an effect on period time of flame oscillation.

(2) Considering vertical temperature in smoke layer (near the wall), the temperature evolutions vary greatly with the level of confinement. In fact, for the same HRR, especailly for HRRs larger than 4.6 kW, in corresponding to equivalence ratio greater than 1, the greater the confinement level is, the lower the temperatures close to the ceiling presents. This variation is associated to the combustion process for different configurations. Besides, correlations of normalized temperature rise for five configurations are proposed.

(3) The higher the confinement level is, the more the area of impinging zone on the ceiling decreases. The maximum ceiling temperature is at the flame impinging point and decreases along the transverse radius of ceiling.

The results in this study may help to design fire detectors on the ceiling and better understand fire behavior and heat transfer during fire disasters in compartments. The hot temperature of unburned gases and a supply of fresh air being the sources of a backdraft, it is desirable to check the temperature level in the enclosure to avoid the fire progress to a backdraft.

In future, the effect of the fire source's position will be studied and the investigation on the full-scale model will be carried out.

Acknowledgements

The authors thank the reviewers for their valuable comments on the initial version of this paper.

References

[1] G. Heskestad, T. Hamada, Ceiling jets of strong fire plumes, Fire Saf. J. 21 (1993) 69–82. https://doi.org/10.1016/0379-7112(93)90005-B.

[2] H.Z. You and G.M. Faeth, An investigation of fire impingement on a horizontal ceiling, 1979.

[3] R.L. Alpert, Calculation of response time of ceiling-mounted fire detectors, Fire Technol. 8 (1972) 181–195. https://doi.org/10.1007/BF02590543.

[4] P.L. Hinkley, H.G.H. Wraight, C.R. Theobald, The contribution of flames under ceilings to fire spread in compartments, Fire Saf. J. 7 (1984) 227–242. https://doi.org/10.1016/0379-7112(84)90022-5.

[5] B. Karlsson, J.G. Quintiere, Enclosure fire dynamics, 2000.

[6] B.J. McCaffrey, Purely buoyant diffusion flames: Some experimental results. National Bureau of Standards Report NBSIR 79-1910., (1979).

[7] R.L. Alpert, Turbulent ceiling-jet induced by large-scale fires, Combust. Sci. Technol. 11 (1975) 197–213. https://doi.org/10.1080/00102207508946699.

[8] D. Gross, Measurement of flame lengths under ceilings, Fire Saf. J. 15 (1989) 31–44. https://doi.org/10.1016/0379-7112(89)90046-5.

[9] X. Zhang, L. Hu, M.A. Delichatsios, J. Zhang, Experimental study on flame morphologic characteristics of wall attached non-premixed buoyancy driven turbulent flames, Appl. Energy. 254 (2019) 113672. https://doi.org/10.1016/j.apenergy.2019.113672.

[10] M. Mann, C. Jainski, M. Euler, B. Böhm, A. Dreizler, Transient flame-wall interactions: Experimental analysis using spectroscopic temperature and CO concentration measurements, Combust. Flame. 161 (2014) 2371–2386. https://doi.org/10.1016/j.combustflame.2014.02.008.

[11] Y. Zhen, B. Lei, H. Ingason, Y.Z. Li, B. Lei, H. Ingason, The maximum temperature of buoyancy-driven smoke flow beneath the ceiling in tunnel fires, Fire Saf. J. 46 (2011) 204–210. https://doi.org/10.1016/j.firesaf.2011.02.002.

[12] J. Ji, C.G. Fan, W. Zhong, X.B. Shen, J.H. Sun, Experimental investigation on influence of different transverse fire locations on maximum smoke temperature under the tunnel ceiling, Int. J. Heat Mass Transf. 55 (2012) 4817–4826. https://doi.org/10.1016/j.ijheatmasstransfer.2012.04.052.

[13] Z.H. Gao, Z.X. Liu, H.X. Wan, J.P. Zhu, Experimental study on longitudinal and transverse temperature distribution of sidewall confined ceiling jet plume, Appl. Therm. Eng. 107 (2016) 583–590. https://doi.org/10.1016/j.applthermaleng.2016.07.007.

[14] A.S. Newale, B.A. Rankin, H.U. Lalit, J.P. Gore, R.J. McDermott, Quantitative infrared imaging of impinging turbulent buoyant diffusion flames, Proc. Combust. Inst. 35 (2015) 2647–2655. https://doi.org/10.1016/j.proci.2014.05.115.

[15] X. Tian, M. Zhong, C. Shi, P. Zhang, C. Liu, Full-scale tunnel fire experimental study of fire-induced smoke temperature profiles with methanol-gasoline blends, Appl. Therm. Eng. 116 (2017) 233–243. https://doi.org/10.1016/j.applthermaleng.2017.01.099.

[16] X. Zhang, L. Hu, W. Zhu, X. Zhang, L. Yang, Flame extension length and temperature profile in thermal impinging flow of buoyant round jet upon a horizontal plate, Appl. Therm. Eng. 73 (2014) 13–20. https://doi.org/10.1016/j.applthermaleng.2014.07.016.

[17] H. Wan, Z. Gao, J. Ji, J. Fang, Y. Zhang, Experimental study on horizontal gas temperature distribution of two propane diffusion flames impinging on an unconfined ceiling, Int. J. Therm. Sci. 136 (2019) 1–8. https://doi.org/10.1016/j.ijthermalsci.2018.10.010.

[18] Z.H. Gao, Z.X. Liu, J. Ji, C.G. Fan, L.J. Li, J.H. Sun, Experimental study of tunnel sidewall effect on flame characteristics and air entrainment factor of methanol pool fires, Appl. Therm. Eng. 102 (2016) 1314–1319. https://doi.org/10.1016/j.applthermaleng.2016.03.025.

[19] M. Poreh, G. Garrad, A Study of wall and corner fire plumes, Fire Saf. J. 34 (2000) 81–98. https://doi.org/10.1016/S0379-7112(99)00040-5.

[20] C. Tao, Y. He, Y. Zhuang, Y. Qian, X. Cheng, X. Wang, The investigation of flame length of buoyancy-controlled gas fire bounded by wall and ceiling, Appl. Therm. Eng. 127 (2017) 1172–1183. https://doi.org/10.1016/j.applthermaleng.2017.08.123.

[21] Z. Gao, J. Jie, H. Wan, J. Zhu, J. Sun, Experimental investigation on transverse ceiling flame length and temperature distribution of sidewall confined tunnel fire, Fire Saf. J. 91 (2017) 371–379. https://doi.org/10.1016/j.firesaf.2017.04.033.

[22] C. Raksmey, X. Zhang, L. Hu, X. Sun, Temperature profile of thermal flow underneath an inclined ceiling induced by a wall-attached fire, Int. J. Therm. Sci. 141 (2019) 133–140. https://doi.org/10.1016/j.ijthermalsci.2019.03.028.

[23] C.G. Fan, J. Yang, Experimental study on thermal smoke backlayering length with an impinging flame under the tunnel ceiling, Exp. Therm. Fluid Sci. 82 (2017) 262–268. https://doi.org/10.1016/j.expthermflusci.2016.11.019.

[24] J. Ji, C.G. Fan, Y.Z. Li, H. Ingason, J.H. Sun, Experimental study of non-monotonous sidewall effect on flame characteristics and burning rate of n-heptane pool fires, Fuel. 145 (2015) 228–233. https://doi.org/10.1016/j.fuel.2014.12.085.

[25] W. Zhao, R. Zong, X. Fan, X. Zhao, Impact of openings on fire properties in the confined corridors, Appl. Therm. Eng. 110 (2017) 746–757. https://doi.org/10.1016/j.applthermaleng.2016.08.206.

[26] J.G. Quintiere, Fundamentals of Fire Phenomena, 2006. https://doi.org/10.1002/0470091150.ch12.

[27] O. Pettersson, S.E. Magnusson, J. Thor, Fire engineering design of steel structures, Stockholm, 1976. https://doi.org/10.1260/1369433054349141.

[28] G. Joulin, Flame oscillations induced by conductive losses to a flat burner, Combust. Flame. 46 (1982) 271–281. https://doi.org/10.1016/0010-2180(82)90021-9.

[29] B. Niu, J. Zhang, J. Wei, Multiple-parameter bifurcation analysis in a Kuramoto model with time delay and distributed shear, AIP Adv. 8 (2018). https://doi.org/10.1063/1.5029512.

[30] J.M. Grier, Combustion: Types of reactions, fundamental processes and advanced technologies, 2014.

[31] S.A. Korpela, Appendix B: Thermodynamic Tables, Princ. Turbomach. (2012) 437–448. https://doi.org/10.1002/9781118162477.app2.

[32] H. Kitahata, J. Taguchi, M. Nagayama, T. Sakurai, Y. Ikura, A. Osa, Y. Sumino, M. Tanaka, E. Yokoyama, H. Miike, Oscillation and synchronization in the combustion of candles, J. Phys. Chem. A. 113 (2009) 8164–8168. https://doi.org/10.1021/jp901487e.

[33] D.J. Rasbash, The S.F.P.E. handbook of fire protection engineering, 1989. https://doi.org/10.1016/0379-7112(89)90011-8.

[34] J. Ji, Y. Fu, K. Li, J. Sun, C. Fan, W. Shi, Experimental study on behavior of sidewall fires at varying height in a corridor-like structure, Proc. Combust. Inst. 35 (2015) 2639–2646. https://doi.org/10.1016/j.proci.2014.06.041.